Polymer Chemistry

ROYAL SOCIETY OF CHEMISTRY

COMMUNICATION

View Article Online
View Journal | View Issue

Check for updates

Cite this: *Polym. Chem.*, 2023, **14**, 4275

Received 10th August 2023,
Accepted 31st August 2023

DOI: 10.1039/d3py00929g

rsc.li/polymers

Amine-bearing cyclic ketene acetals for pH-responsive and degradable polyesters through radical ring-opening polymerisation†

Yiyi Deng, [a,b] Anaïs Frezel,[a,b] Fabian Mehner, [a,b] Peter Friedel [a] and Jens Gaitzsch *[a]

A series of previously unreported amine-bearing cyclic ketene acetals (CKAs) furnished with different alkyl-substituents were prepared. These CKAs pave the way for a new range of pH-responsive and degradable polyesters from radical ring-opening polymerisation (RROP). CKA 2-methylene-1,3,6-trioxocane (MTC) was co-polymerised with the amine-bearing CKAs to obtain a range of new degradable smart copolymers. Varying the type and amount of amine-bearing CKA allowed to fine-tune the pK_a^* value of the polymers, showcasing the versatility of this approach.

Following the increasing issues with plastic waste, polyesters like poly(caprolactone) (PCL) or poly(lactic acid) (PLA) and similar materials have become increasingly important materials owing to the biodegradable ester units in the polymer backbone. They found numerous applications in tissue engineering, drug delivery or commodity materials.[1] Traditional synthetic routes towards polyesters are either by polycondensation or ring-opening polymerisation.[2] However, the former tends to generate polyesters with low molecular weight and the latter method requires rigorous synthetic procedures (especially from ionic polymerization) to afford pure polymers.[3] Proposed by Bailey *et al.*, radical ring-opening polymerisation (RROP) of cyclic ketene acetals (CKAs) has received considerable attention and is regarded as an alternative tool to generate polyesters.[4] RROP possesses the robustness of radical polymerisations, yields degradable polyesters[2,5] and allows for functional groups (*e.g.* amines) within the polymer backbone.[6]

Homopolymerisations of CKAs are known to generate polyesters (bio)degrading under basic or enzymatic conditions.[7,8] Until now, 2-methylene1,3-dioxepane (MDO), 2-methylene-1,3,6-trioxocane (MTC) and 2-methylene-4-phenyl-1,3-dioxolane (MPDL) are the CKAs with be highest publication record.[9–13] These CKAs are generally characterised by an almost complete degree of ring-opening and a known structure in terms of the main repeating unit and branching positions from inter- or intramolecular H-transfer.[13–16] Some of these polymers already have an additional functionality like the semi-crystallinity of poly(MDO) and the higher hydrophilicity of poly(MTC) as compared to other polyesters from RROP.[12–14] However, the lack of responsive groups limits their range of potential applications like drug delivery.[17]

One strategy to circumvent this issue is the copolymerisation of CKAs with various responsive vinylic monomers.[5,18–20] This strategy introduced ester linkages into the vinyl polymer backbone to confer (bio)degradability[2] and responsive vinylic monomers endowed responsive properties.[21,22] CKAs including MDO and BMDO have been successfully combined with oligoethylene glycol methacrylate and *N*,*N*-dimethylacrylamide for water solubility,[23–25] *N*-isopropylacrylamide for temperature responsiveness[26,27] and 2-(diethylamino)ethyl methacrylate for pH-responsivness.[23,28] CKA-bearing copolymers have been developed in the field of functional and degradable nanoparticles,[29–31] hydrogels,[32] 3D printing materials,[33] and coatings.[34,35] However, the unfavorable CKA/vinylic copolymerisation parameters caused a composition drift towards gradient copolymer, which prohibited the randomly distributed ester units in the polymer backbone. This will therefore lead to an incomplete degradation into a mixture of oligomers.[36,37] Hence, a reproducible method towards responsive and fully degradable polyesters from RROP is still a challenge.

Our group has focused on fully degradable polyesters purely based on CKAs,[6,8,15,38] including amine-bearing CKAs for pH-responsive polyesters. This includes the amine-bearing *N*-iso-propyl-2-methylene-1,3,6-dioxazocane (^{i}Pr-MAC, **7c**), allowing for pH-responsive and biodegradable nanoparticles.[6] With a cloud point of 6.0, the pK_a of the polymerised ^{i}Pr-MAC was similar to the well-known pH-responsive poly(diisopropyl aminoethyl methacrylate) (PDPA).[39] Copolymerisation of **7c** ^{i}Pr-MAC with 4,7-dimethyl-2-methylene-1,3-dioxepane (DMMDO) led to copolymers with an increased molecular weight, but the pH-

[a]*Leibniz-Institut für Polymerforschung Dresden e.V., Hohe Straße 6, 01069 Dresden, Germany. E-mail: gaitzsch@ipfdd.de*
[b]*Technische Universität Dresden, Berg Straße 66, 01069 Dresden, Germany*
† Electronic supplementary information (ESI) available. See DOI: https://doi.org/10.1039/d3py00929g

responsive behaviour shifted from 6 for P(^{i}Pr-MAC) to below 4 for the copolymer. Taking advantage of these merits, *i.e.*, pH-sensitivity and biodegradability, these purely CKA-based polyesters and nanoparticles accessed potentials in biomedical field, but lacked a pK_a value closer to neutral pH. Inspired by this notion, we adopted the reported synthetic route to prepare new amine-bearing CKAs with varying substituents (Alk-MACs), including the ethyl (Et-MAC, **7a**), *n*-propyl (^{n}Pr-MAC, **7b**), *n*-butyl (^{n}Bu-MAC, **7d**), *sec*-butyl (^{s}Bu-MAC, **7e**), iso-butyl (^{i}Bu-MAC, **7f**) and *tert*-butyl (^{t}Bu-MAC, **7g**) derivatives (Fig. 1a). Following monomer synthesis and calculations on the molecule structure, we subsequently copolymerised the Alk-MACs with the more hydrophilic MTC as it ought to have a pK_a closer to neutral pH (Fig. 1b). Hydrolytic degradation will be briefly discussed as well (Fig. 1c).

The first goal of this work was to synthesise the new Alk-MACs following a similar protocol (carbonate route) as for the published ^{i}Pr-MAC. Starting from diethanolamine **1**, alkyl-substituted diols **3** were prepared by alkylation with the corresponding bromoalkene agents **2**. Following some optimisation, the previously reported *N*-propyldiethanolamine **3b**, *N*-iso-propyldiethanolamine **3c**, *N*-*sec*-butyldiethanolamine **3e** and also *N*-iso-butyldiethanolamine **3f** were synthesised (Tables S2–S5 and Fig. S3†). The substances **3a**, **3d**, and **3g** were sourced commercially.

These alkyl-modified diols **3a–g** and ethyl chloroformate **4** then reacted in the presence of triethylamine (TEA) to yield the intermediate cyclic carbonates **5a–g**. Reaction conditions, including reaction temperature, feeding speed of TEA, feed ratio of reagents, were fine-tuned individually to ensure optimal yield of each carbonate. For instance, the best yield of ethyl carbonate **5a** (23%) was achieved with a low feeding speed of TEA (15 μL min^{-1}). Conversely, a faster feeding speed of TEA (40 μL min^{-1}) gave the best yield for *n*-propyl carbonate **5b** and *tert*-butyl carbonate **5g** with 29% each. An even higher feeding speed of 100 μL min^{-1} then gave the optimal yield of 45% for *sec*-butyl carbonate **5e** and was increased further to 400 μL min^{-1} for the formation of *n*-butyl carbonate **5d** (25% yield) and iso-butyl carbonate **5f** (45% yield, summarized in Tables S6–11†). Hence, larger alkyl substituents mostly demanded a higher feeding speed of TEA for optimal carbonate formation. ^{1}H NMR and ^{13}C NMR spectroscopy with full signal assignment could be achieved for all carbonates **5a–g**, always including the signal at around 155 ppm in the ^{13}C NMR, (carbonate-bearing carbon atom). HR-ESI-MS measurements with positive mode were used to confirm the successful synthesis of all cyclic carbonates **5a–g** (Fig. S4–10†). Molecular models were calculated to get insights into the geometry of the structures (Fig. S20†) and will be discussed separately later.

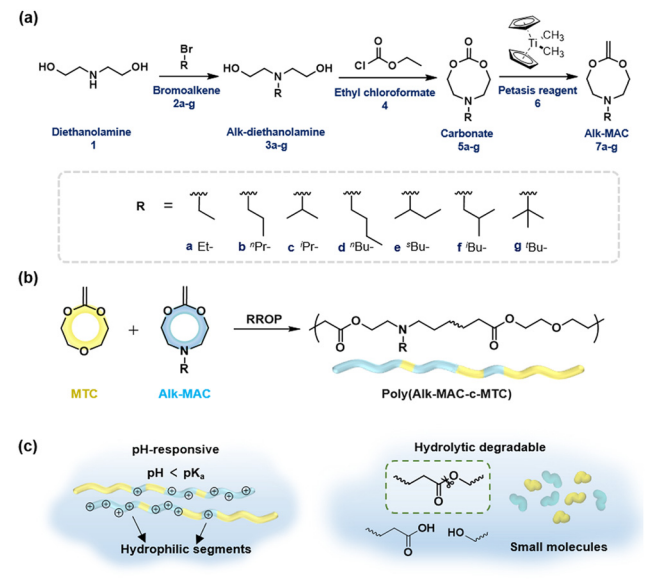

Fig. 1 (a) Synthetic route towards Alk-MACs through an intermediate carbonate. Labels **3a–g**, **5a–g**, **7a–g** represent alkyl-substituted diethanol amines, intermediate carbonates and CKAs, respectively. (b) Copolymerisation of Alk-MACs with the conventional CKA MTC yields pH-responsive and degradable copolymers. (c) The amines in the Alk-MAC segments get protonated upon acidification and copolymers become hydrophilic and upon hydrolytic degradation the ester bonds get cleaved to yield small molecules.

Methylenation of all cyclic carbonates **5a–g** (1.0 equiv.) with the Petasis reagent **6** (2.3 equiv.) were performed in THF at 65 °C for 22 h. All the new CKAs were obtained in a low yield (from 6% for **7d** over 11–15% for **7a–b**, **7e–g** to 25% for **7c** (Table S1†)), representing the delicacy of the carbonate route. ^{1}H, ^{13}C NMR and HR-ESI-MS measurements confirmed the successful preparation of these new molecules (Fig. 2 and Fig. S12–18†). As depicted in Fig. 2, signals **a–d** could be assigned to the CKA ring. From the core CKA functionality, the tertiary carbon atom **c** between the oxygen atoms was positioned at 164 ppm for the ^{13}C NMR spectrum (Fig. S12–S18†). The intense singlet **d** in the range of 3.53–3.61 ppm in the ^{1}H NMR spectra and new signal at 69 ppm in the ^{13}C NMR spectra represented *exo*-methylene group and hence proved the formation of the MACs. Signals **1–4** were attributed to the protons on the alkyl-substituents and remained mainly unchanged from the carbonates for all substituents. As compared to other chemical shifts of the starting diols and intermediate substances, protons **a**, **a′** and **2**, **2′** of the chiral ^{s}Bu-MAC **7e** and the corresponding carbonate **5e** showed an additional splitting (see in Fig. 2 and S8†), which is typical for chiral molecules.

Additionally, theoretical calculations of the molecular structures of all intermediate carbonate and corresponding CKAs were performed using software package GAMESS with basis set STO-6G,[40] simulating conditions of 0 K and vacuum. These helped us in understanding the energetically optimal structure of the carbonates **5a–g** and CKAs **7a–g** (see in the insets in Fig. 2 and Fig. S20†). They revealed that, except for the chiral ^{s}Bu derivatives **5e** and **7e**, the side chain on the amine stretched away from the carbonate or CKA ring. Both chiral derivatives, however, presented an additional structural distinctiveness. Here, the ^{s}Bu-side group tended to bend inwards to the eight-membered ring, which might lead to significant steric hindrance around the tertiary amine. However, as the

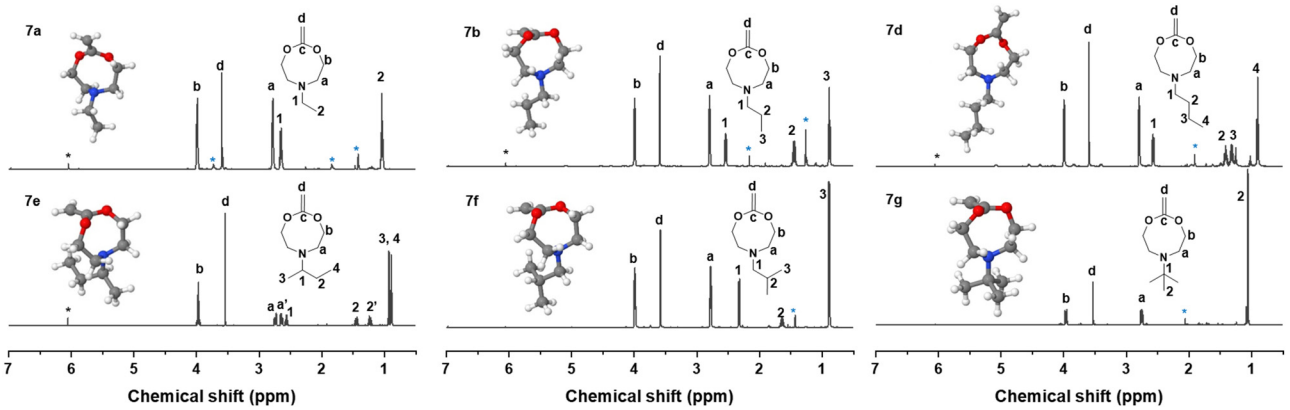

Fig. 2 ^{1}H NMR spectra of all new Alk-MACs **7a–b**, **7d–g** with their respective alkyl side groups. The inserts are energetic optimal structures of CKAs calculated at 0 K, under vacuum; red balls represent oxygen atoms, grey balls represent carbon atoms, white balls represent hydrogen atoms, blue balls represent nitrogen atoms. The asterisked signals in the ^{1}H NMR spectra represent the trace of Petasis reagent (black, 6.05 ppm), solvent and impurities (blue, *tert*-butanol: 1.28 ppm, acetone: 2.17 ppm, THF: 1.85 and 3.76 ppm).

calculations were performed at simulated 0 K, the effect on the molecule at room temperature remained unknown.

Copolymerisation of the previously reported ^{i}Pr-MAC **7c** and conventional CKA MTC was the starting point to fabricate the pH-responsive polyesters through free RROP. By varying feed ratio of **7c** to MTC from 5/95, 10/90, 25/75 to 50/50 (mol%), copolymer composition was modulated. After polymerising either thermally or under UV light for 24 h, purified copolymers were obtained through dialysis. All copolymers were named according to the feed ratio of Alk-MACs and the polymerisation method. For instance, ^{i}Pr-MAC-5T represents a **7c**/MTC mixture with a feed ratio of 5/95 that was subjected to thermal polymerisation.

To determine the monomer conversion and the final molar fractions, crude and purified copolymers were analysed by ^{1}H NMR spectroscopy (Fig. S21–24†). Signals attributed to protons on the P(MTC) parts were consistent with reported signal assignments.[14] For the P(^{i}Pr-MAC) segment, the signal centered at 2.93 ppm appeared in all the samples, which is attributed to the α-proton on the ^{i}Pr side chain. This signal was significant, as the chemical shift remained virtually unchanged for the monomer and the polymer and confirmed the successful incorporation of the ^{i}Pr group through all attempts. After workup, the ester signal of P(MTC) (4.20 ppm) and amine signal of P(^{i}Pr-MAC) (2.93 ppm) were integrated to calculate the molar fractions in the copolymers (Fig. S23 and section 3.3 of the ESI†). Intriguingly, the final molar fraction of ^{i}Pr-MAC in the copolymers was always higher than the feed ratio, indicating that ^{i}Pr-MAC was more reactive than MTC. Additionally, UV-irradiated polymerisation consistently led to a higher ^{i}Pr-MAC content in the copolymers as compared to thermal polymerization, implying an even greater imbalance of reactivities (Table 1). Copolymers of ^{i}Pr-MAC and MTC could hence be gradient copolymers, which means copolymers first enriched with ^{i}Pr-MAC. Considering the omnipresent dispersity within polymers from free radical polymerisation, the partial presence of homopolymers could not be excluded. DOSY measurements of the bimodal copolymer ^{i}Pr-MAC-5T was carried out (Fig. S26†), and showed that the self-diffusion coefficients related to ^{i}Pr-MAC and MTC motifs within the main diffusion peak and thus substantiated the successful formation of a copolymer. Additionally, MTC branching units occurred by intramolecular (MTC back-biting) or intermolecular H-abstraction reactions can also be observed. The characteristic signals around 1.20 ppm are related to the methyl end groups from each MTC branching unit (Fig. S24†).[13,41] The SEC chromatograms of the resultant copolymers showed that with increasing ^{i}Pr-MAC content, copolymers exhibited a broader distribution ranging from 1.3 for 5 mol% to over 11 for 50 mol% (Fig. S29† and Table 1). While thermal initiation showed a consistent increase in dispersity with rising ^{i}Pr-MAC content, tendency was less clear for polymerizations under UV irradiation, again implying a more reliable reaction under purely thermal conditions. The corresponding results should be treated with caution owing to the complex polymeric structures including ring-opened and ring-retaining structures as well as branched and linear units in all possible combinations from MTC and ^{i}Pr-MAC. 2D NMR measurements of sample copolymers (Fig. S27 and 28†) still allowed for allocating some major signals. As the ester bonds of MTC and the amines of ^{i}Pr-MAC could be confirmed, both structural arguments for the targeted degradability and pH-responsiveness were present.

Following the more reliable reaction, thermal polymerisation was applied to other Alk-MAC/MTC pairs. A feed ratio of 25/75 (mol%, Alk-MAC/MTC) was applied to yield an Alk-MAC content between 25 and 50 mol% as this would ensure pH-responsiveness and also the MTC content necessary to keep structural diversity within reason. The purified copolymers were analysed by ^{1}H- and ^{13}C NMR spectroscopy and are comprised in Fig. S32–S33.† Similar to the ^{i}Pr-MAC/MTC copolymers, the high amount of possible substructures prohibited

Table 1 Experimental conditions of copolymerisation of MTC with Alk-MACs and the composition of resultant copolymers

Name	$f_{MAC,0}/f_{MTC,0}$ [a]	% Conv. MAC/MTC[b]	F_{MAC}/F_{MTC} [c]	M_n [d] (kg mol^{-1})	M_w [d] (kg mol^{-1})	$Đ$[d]	pK_a^* [e]
^{i}Pr-MAC-5T	5/95	67/35	7/93	25.8	32.9	1.3	—
^{i}Pr-MAC-10T	10/90	40/28	14/86	26.6	43.5	1.6	—
^{i}Pr-MAC-25T	25/75	48/25	34/66	32.2	155	4.8	7.0 ± 0.1
^{i}Pr-MAC-50T	50/50	35/37	69/31	18.2	193	11	6.5 ± 0.1
^{i}Pr-MAC-5U	5/95	80/67	10/90	16.3	47.4	2.9	—
^{i}Pr-MAC-10U	10/90	100[f]/38	19/81	29.3	68.2	2.3	—
^{i}Pr-MAC-25U	25/75	64/15	55/45	9.2	31.5	3.4	6.9 ± 0.2
^{i}Pr-MAC-50U	50/50	100[f]/44	80/20	16.5	248	15	6.7 ± 0.2
Et-MAC-25T	25/75	22/17	37/63	17.8	44.8	2.5	5.7 ± 0.3
^{n}Pr-MAC-25T	25/75	27/26	26/74	15.3	42.4	2.8	6.1 ± 0.2
^{n}Bu-MAC-25T	25/75	22/17	36/64	11.8	126	11	6.6 ± 0.3
^{s}Bu-MAC-25T	25/75	29/13	45/55	49.1	420	8.6	6.6 ± 0.3
^{i}Bu-MAC-25T	25/75	30/17	30/70	21.5	183	8.5	6.4 ± 0.2
^{t}Bu-MAC-25T	25/75	60/19	50/50	10.8	65.4	6.1	7.2 ± 0.3

[a] Feed ratios of Alk-MACs to MTC. [b] Conversion of Alk-MACs and MTC, calculated by ^{1}H NMR spectra. [c] Final molar fraction of Alk-MACs to MTC in the resulting copolymers, calculated from ^{1}H NMR spectra. [d] M_n, M_w and polymer dispersity were measured by SEC at 25 °C with a PolarGel-M column (300 × 7.5 mm), using HPLC-Pump 1200 pump system (Agilent technologies) equipped with a multi angle laser light scattering (MALLS) detector (MiniDAWN TREOS II, Wyatt Technology) and a RI detector (K-2301 from KNAUER). DMAc with 3 g L^{-1} LiCl was used as an eluent and the flow rate was 1 mL min^{-1}. [e] pK_a^* was obtained through UV-vis method, the transition point was determined when transmittance decreased 50%. It should be noted that pK_a^* shown in the Table 1 was the average value obtained from three measurements, including the corresponding error margin. [f] Conversion of Alk-MACs was quite high and no presence of vinyl protons can be found by ^{1}H NMR spectra.

complete signal assignment and hence also quantification of the degree of ring-opening. Branching from MTC units could be confirmed in all cases from the aforementioned signals around 1.20 ppm, but was not quantified due to signal overlap (Fig. S32†). Ester linkages within the copolymer were further confirmed by an exemplary ATR-FTIR spectrum of Et-MAC-25T (Fig. S34†). It showed a strong band 1734 cm^{-1}, showcasing the stretching vibration of the C=O bonds of ester units. The Alk-MAC/MTC content could still be determined as characteristic signals for MTC and the alkyl-substituents on the MACs could be attributed (Table 1 and Fig. S30–31†). Final molar ratios of Alk-MACs/MTC were higher than the feed ratio, highlighting the higher reactivity of all investigated Alk-MACs compared to MTC, again suggesting the formation of gradient copolymers. SEC measurements of all copolymers showed a somewhat constant M_n of 15.4 ± 4.5 kg mol^{-1} (Fig. S35† and Table 1). Only ^{s}Bu-MAC-25T showed a higher M_n of 49.1 kg mol^{-1}. While Et-MAC-25T and ^{n}Pr-MAC-25T copolymers had relatively reasonable dispersity values of 2.5 and 2.8, these values went up to 4.8 for ^{i}Pr-MAC-25T and rose further to 6–11 for the butyl derivatives. It indicated a lack of control over dispersity with increasing length and complexity of the side chain on the amine. A suspected reason for this could be the additional branching sites on the side chain, especially close to the amines. These new propagation centres could then themselves host new polymer chains with branches from all different branching points, leading to a plethora of possible sub-structures and also increased dispersities.

All copolymers contained the aimed-for amount of Alk-MAC and pH-responsiveness was then characterised by dissolving each copolymer in a HCl solution, titrating it from pH 2 towards pH 10. This process deprotonated the ammonium units and gave tertiary amines, changing the solubility of the copolymers from hydrophilic (transparent solution) to hydrophobic (turbid solution) (Fig. 3a). Turbidity pointed towards aggregation and DLS measurement of ^{i}Pr-MAC-25T/HCl at different pH values confirmed this (Fig. S46†). Volume size distribution traces showed significant increases in hydrodynamic size and polydispersity index (PDI) upon deprotonation, proofing the formation of agglomerates during this process. Turbidity measurements then showed a reversible deprotonation–protonation and hence transparent-turbidity switch of ^{i}Pr-MAC-25T over three cycles between pH 3 and 10 (Fig. 3b). The titration plots of % transmittance against pH value were then measured at a wavelength of 500 nm and then fitted with a Boltzmann equation (in Fig. S36–45†). When transmittance decreased to 50% of the original value, this pH was defined as pK_a^* cloud point. Copolymer solutions of all substituents were measured as triplicates and first evaluated separately in order to get mean values and error margins (Fig. S36–45† left side, values in Table 1). In a second instance, the values of all three measurements were fitted together in a single Boltzmann fit in order to compare different substituents against each other (Fig. S36–45† right side, comparison in Fig. 3c–e). Within these studies, M_n values were within reason and dispersity values were found to have no measurable impact on this value. Subsequently, impact on the pK_a^* was analysed for (i) amount of Alk-MAC in the polymer, (ii) length of Alk-MAC substituent, (iii) bulkiness of Alk-MAC substituent. For the first category, copolymers with different amounts of ^{i}Pr-MAC were compared (Fig. 3c). Within this series, the pK_a^* dropped from 7.1 for 34% of ^{i}Pr-MAC (^{i}Pr-MAC-25T) to 6.6 for 69% of ^{i}Pr-MAC (^{i}Pr-MAC-50T). Only the pK_a^* of 6.7 for 80% ^{i}Pr-MAC-50U does not perfectly fit this trend, but this could be explained with increasing structural irregularities following the low MTC content. In our previous research, the ^{i}Pr-MAC homopolymer exhibited a pK_a value around 6.0.[6] All pK_a^* cloud-point values are within the same region, but cannot be compared directly

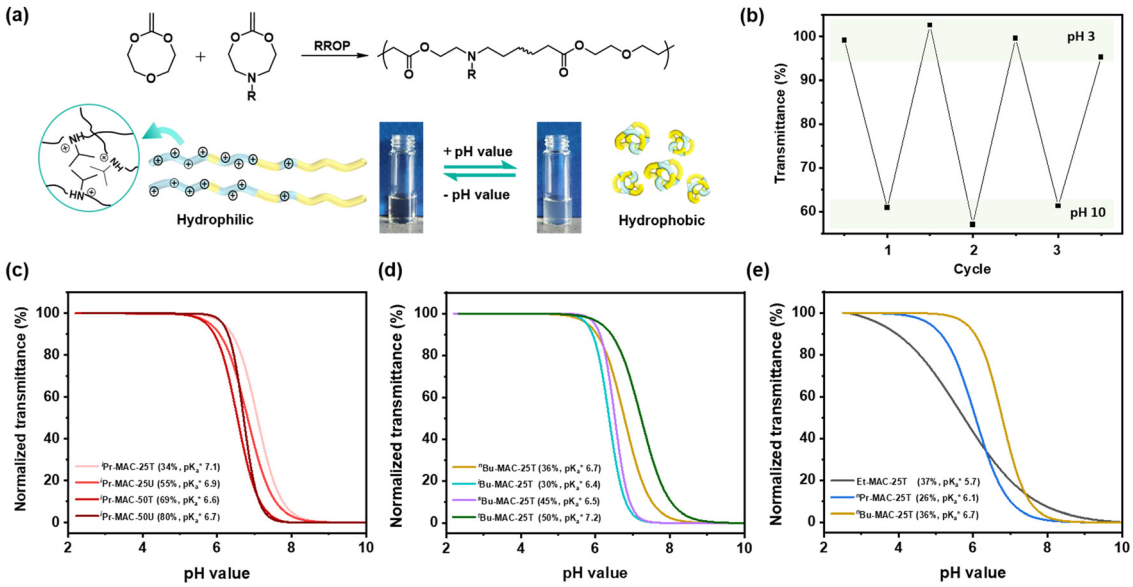

Fig. 3 (a) Transparent copolymer solutions became turbid when the pH value increased. (b) Reversible deprotonation–protonation process of ^{i}Pr-MAC-25T copolymer solution detected by UV-Vis measurements over three cycles. (c)–(e) Evolution of % transmittance of copolymers solution over pH, showing dependencies of (c) amount of incorporated ^{i}Pr-MAC, (d) bulkiness of the butyl substitute (^{n}Bu, ^{i}Bu, ^{s}Bu, ^{t}Bu), (e) length of the *n*-alkyl substituent (Et, ^{n}Pr, ^{n}Bu). The pK_a^* values shown in the figure caption were obtained from the single Boltzmann fit of all three measurements of respective copolymer, and therefore were slightly different from the average pK_a^* value listed in the Table 1 (for a comparison of both values, see Table S13 in the ESI†).

following the different measurement principles. Owing to the higher hydrophilicity of MTC, all pK_a^* values were considerably higher than the one recorded for the ^{i}Pr-MAC/DMMDO copolymer (found at pH 3.5),[6,13,14] meeting a major goal of this study.

For all Bu-MAC copolymers (Fig. 3d), the MAC content ranged from 30% in ^{i}Bu-MAC-25T to 50% in ^{t}Bu-MAC-25T, being in a comparable range. The bulkiest residue of ^{t}Bu-MAC-25T exhibited the highest pK_a^* of 7.2 despite having the highest amount of Bu-MAC units. All three other Bu-MACs were relatively close to each other with pK_a^* values of 6.4, 6.5 and 6.7 for ^{i}Bu-MAC-25T, ^{s}Bu-MAC-25T and ^{n}Bu-MAC-25T, respectively. This implicated that the steric hindrance of the ^{t}Bu residue caused this higher pK_a^* value.

Copolymers with linear substituents showed that Et-MAC-25T exhibited a significantly broader reduction region of % transmittance than ^{n}Pr-MAC-25T and ^{n}Bu-MAC-25T. As molecular weights remained within reason, this change could be attributed to the length of the side chain. Corresponding pK_a^* values increased from 5.7 for Et-MAC-25T over 6.1 for ^{n}Pr-MAC-25T to 6.7 for ^{n}Bu-MAC-25T. It can hence be concluded that longer alkyl substituents promoted a higher pK_a^* value. This could again be attributed to the increasing steric hindrance of a larger substituent, which goes in-line with the shift of the pK_a^* values observed within the series of butyl-substituents.

Selected copolymers were then subjected to hydrolytic degradation under accelerated condition. The copolymers were dissolved in THF/MeOH (67/33 vol%) with 5 wt% KOH and kept stirring at room temperature for 24 h to ensure complete degradation. Degradation was then proven in multiple ways: (i) ^{1}H NMR measured in $CDCl_3$ and D_2O: signals around 4.2 ppm

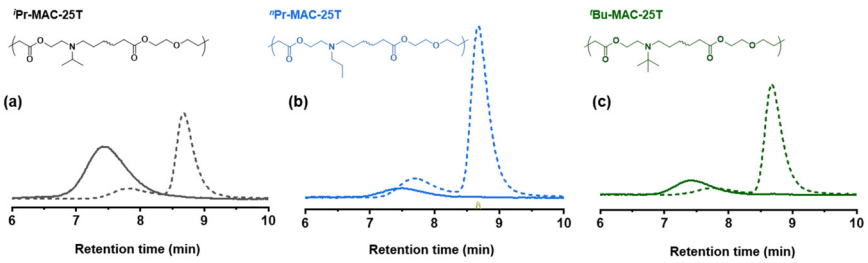

Fig. 4 SEC analysis of copolymers before (solid lines) and after hydrolytic degradation (dashed lines) under accelerated conditions. Light scattering signals of (a) ^{i}Pr-MAC-25T, (b) ^{n}Pr-MAC-25T and (c) ^{t}Bu-MAC-25T are depicted.

ascribed to the protons adjacent to ester bond of P(MTC) disappeared completely after degradation (Fig. S47 and S49†). (ii) ^{13}C NMR: signals around 174 ppm (Fig. S48†), related to carbon atoms in ester bond, also disappeared. (iii) SEC: similar to other RROP studies,[13,29] chromatograms before and after degradation showed a significant shift towards higher retention time after degradation for 24 h (Fig. 4 and Fig. S50†). Altogether, this confirmed the degradation of the copolymers.

Conclusions

We hence successfully synthesized a series of alkyl-substituted Alk-MACs and provided their calculated molecular structures. Copolymerisation of all Alk-MACs with MTC yielded pH-responsive polyesters best under thermal conditions. The pK_a^* cloud point values varied from 5.7 to 7.2 with all the amount, length and bulkiness of the alkyl residue impacting the cloud points. Degradation of selected polyesters could then be proven by the disappearance of characteristic ^{1}H and ^{13}C NMR signals as well as characteristic shifts in the SEC chromatograms. All presented Alk-MACs are thus a valuable addition to heteroatom-bearing CKA library and copolymerisation with MTC is a facile platform to gain pH-responsive and degradable polyesters.

Author contributions

Yiyi Deng: conceptualisation, formal analysis, investigation, data curation, writing – original draft, writing – review and editing, visualisation, funding acquisition. Anais Frezel: validation, formal analysis, investigation, writing – review and editing, visualisation. Fabian Mehner: validation, formal analysis, investigation, writing – review and editing, visualisation. Peter Friedel: methodology, software, investigation, data curation, writing – review and editing, visualisation. Jens Gaitzsch: conceptualisation, methodology, formal analysis, resources, data curation, writing – original draft, writing – review and editing, supervision, project administration, funding acquisition.

Conflicts of interest

There are no conflicts to declare.

Acknowledgements

The manuscript was written by contributions from all authors and all authors gave their approval for the final version. We would like to thank Alissa Seifert for the SEC measurements and Albena Lederer for helpful discussions of the results. The authors thank the Chinese Scholarship Council for funding Y. D., the Evonik Foundation for funding F. M. and the Deutsche Forschungsgemeinschaft (GA2051/7-1) for financial support. We thank the Howdle group at the University of Nottingham for granting access to their NMR facilities.

References

1 D. Goldberg, *J. Environ. Polym. Degrad.*, 1995, **3**, 61–67.
2 S. Agarwal, *Polym. Chem.*, 2010, **1**, 953–964.
3 J. N. Hoskins and S. M. Grayson, *Polym. Chem.*, 2011, **2**, 289–299.
4 W. J. Bailey, Z. Ni and S.-R. Wu, *J. Polym. Sci., Part A: Polym. Chem.*, 1982, **20**, 3021–3030.
5 T. Pesenti and J. Nicolas, *ACS Macro Lett.*, 2020, **9**, 1812–1835.
6 J. Folini, C.-H. Huang, J. C. Anderson, W. P. Meier and J. Gaitzsch, *Polym. Chem.*, 2019, **10**, 5285–5288.
7 G. Hedir, C. Stubbs, P. Aston, A. P. Dove and M. I. Gibson, *ACS Macro Lett.*, 2017, **6**, 1404–1408.
8 J. Gaitzsch, P. C. Welsch, J. Folini, C.-A. Schoenenberger, J. C. Anderson and W. P. Meier, *Eur. Polym. J.*, 2018, **101**, 113–119.
9 M. R. Hill, T. Kubo, S. L. Goodrich, C. A. Figg and B. S. Sumerlin, *Macromolecules*, 2018, **51**, 5079–5084.
10 J. Tran, E. Guégain, N. Ibrahim, S. Harrisson and J. Nicolas, *Polym. Chem.*, 2016, **7**, 4427–4435.
11 M. R. Hill, E. Guégain, J. Tran, C. A. Figg, A. C. Turner, J. Nicolas and B. S. Sumerlin, *ACS Macro Lett.*, 2017, **6**, 1071–1077.
12 F. Mehner, M. Geisler, K. Arnhold, H. Komber and J. Gaitzsch, *ACS Appl. Polym. Mater.*, 2022, **4**, 7891–7902.
13 T. Pesenti, E. Gillon, S. Ishii, S. Messaoudi, Y. Guillaneuf, A. Imberty and J. Nicolas, *Biomacromolecules*, 2023, **24**, 991–1002.
14 J. Undin, P. Plikk, A. Finne-Wistrand and A.-C. Albertsson, *J. Polym. Sci., Part A: Polym. Chem.*, 2010, **48**, 4965–4973.
15 Y. Deng, F. Mehner and J. Gaitzsch, *Macromol. Rapid Commun.*, 2023, **44**, 2200941.
16 A. Tardy, J. Nicolas, D. Gigmes, C. Lefay and Y. Guillaneuf, *Chem. Rev.*, 2017, **117**, 1319–1406.
17 V. Delplace and J. Nicolas, *Nat. Chem.*, 2015, **7**, 771–784.
18 A. Tardy, J.-C. Honoré, J. Tran, D. Siri, V. Delplace, I. Bataille, D. Letourneur, J. Perrier, C. Nicoletti, M. Maresca, C. Lefay, D. Gigmes, J. Nicolas and Y. Guillaneuf, *Angew. Chem., Int. Ed.*, 2017, **56**, 16515–16520.
19 Y. Zhang, M. Zheng, T. Kissel and S. Agarwal, *Biomacromolecules*, 2012, **13**, 313–322.
20 T. Pesenti, C. Zhu, N. Gonzalez-Martinez, R. M. F. Tomás, M. I. Gibson and J. Nicolas, *ACS Macro Lett.*, 2022, **11**, 889–894.
21 J. Tran, T. Pesenti, J. Cressonnier, C. Lefay, D. Gigmes, Y. Guillaneuf and J. Nicolas, *Biomacromolecules*, 2019, **20**, 305–317.
22 A. Bossion, C. Zhu, L. Guerassimoff, J. Mougin and J. Nicolas, *Nat. Commun.*, 2022, **13**, 2873.

23 U. Wais, L. R. Chennamaneni, P. Thoniyot, H. Zhang and A. W. Jackson, *Polym. Chem.*, 2018, **9**, 4824–4839.
24 J.-F. Lutz, J. Andrieu, S. Üzgün, C. Rudolph and S. Agarwal, *Macromolecules*, 2007, **40**, 8540–8543.
25 S. Komatsu, T. Sato and A. Kikuchi, *Polym. J.*, 2021, **53**, 731–739.
26 D. J. Siegwart, S. A. Bencherif, A. Srinivasan, J. O. Hollinger and K. Matyjaszewski, *J. Biomed. Mater. Res., Part A*, 2008, **87**, 345–358.
27 T.-A. Asoh, T. Nakajima, T. Matsuyama and A. Kikuchi, *Langmuir*, 2015, **31**, 6879–6885.
28 A. W. Jackson, L. R. Chennamaneni and P. Thoniyot, *Eur. Polym. J.*, 2020, **122**, 109391.
29 C. Zhu, S. Denis and J. Nicolas, *Chem. Mater.*, 2022, **34**, 1875–1888.
30 C. Zhu and J. Nicolas, *Polym. Chem.*, 2021, **12**, 594–607.
31 E. Guégain, C. Zhu, E. Giovanardi and J. Nicolas, *Macromolecules*, 2019, **52**, 3612–3624.
32 Y. Hiraguri, K. Katase and Y. Tokiwa, *J. Macromol. Sci., Part A: Pure Appl. Chem.*, 2006, **43**, 1021–1027.
33 M. Carlotti, O. Tricinci and V. Mattoli, *Adv. Mater. Technol.*, 2022, **7**, 2101590.
34 X. Ai, J. Pan, Q. Xie, C. Ma and G. Zhang, *Polym. Chem.*, 2021, **12**, 4524–4531.
35 Q. Xie, Q. Xie, J. Pan, C. Ma and G. Zhang, *ACS Appl. Mater. Interfaces*, 2018, **10**, 11213–11220.
36 D. Gigmes, P. H. M. Van Steenberge, D. Siri, D. R. D'hooge, Y. Guillaneuf and C. Lefay, *Macromol. Rapid Commun.*, 2018, **39**, 1800193.
37 A. Tardy, N. Gil, C. M. Plummer, D. Siri, D. Gigmes, C. Lefay and Y. Guillaneuf, *Angew. Chem., Int. Ed.*, 2020, **59**, 14517–14526.
38 J. Folini, W. Murad, F. Mehner, W. Meier and J. Gaitzsch, *Eur. Polym. J.*, 2020, **134**, 109851.
39 J. Gaitzsch, X. Huang and B. Voit, *Chem. Rev.*, 2016, **116**, 1053–1093.
40 M. W. Schmidt, K. K. Baldridge, J. A. Boatz, S. T. Elbert, M. S. Gordon, J. H. Jensen, S. Koseki, N. Matsunaga, K. A. Nguyen, S. Su, T. L. Windus, M. Dupuis and J. A. Montgomery Jr., *J. Comput. Chem.*, 1993, **14**, 1347–1363.
41 F. Mehner, T. Meissner, A. Seifert, A. Lederer and J. Gaitzsch, *J. Polym. Sci.*, 2023, **61**, 1882–1892.